One-dimensional Markovian-field Ising model: physical properties and characteristics of the discrete stochastic mapping

1988 J. Phys. A: Math. Gen. 21 2151

(http://iopscience.iop.org/0305-4470/21/9/028)

J. Phys. A: Math. Gen. **21** (1988) 2151-2165. Printed in the UK

One-dimensional Markovian-field Ising model: physical properties and characteristics of the discrete stochastic mapping

Ulrich Behn† and Valentin A Zagrebnov‡

† Sektion Physik, Karl-Marx-Universität Leipzig, DDR-7010 Leipzig, German Democratic Republic

‡ Laboratory of Theoretical Physics, Joint Institute for Nuclear Research, Dubna 141980, USSR

Received 2 October 1987, in final form 21 January 1988

Abstract. The zero-temperature physical properties of an Ising chain in a Markovian field taking only two values with non-zero mean are evaluated and a related discrete stochastic mapping with the theory of finite Markov chains is investigated. A discontinuous behaviour of the magnetisation and the residual entropy, dependent on both mean field and exchange, is found which can be related to flips of microscopic spin clusters. For non-zero temperature the mapping is characterised by the fractal properties of its attractor and by the Lyapunov exponent. An explicit expression for the measure in the nth iteration of the Chapman-Kolmogorov equation is obtained.

1. Introduction

The calculation of the partition function of the one-dimensional Ising model in an external static random magnetic field h_n can be reduced to the problem of *one* spin in an auxiliary local random field [1, 2]

$$Z^N = \sum_{\{s_n\}} \exp\left(\beta \sum_{n=1}^{N} (Js_n s_{n+1} + h_n s_n)\right)$$
$$= \sum_{s_N} \exp\left[\beta\left(\xi_N s_N + \sum_{n=1}^{N-1} B(\xi_n)\right)\right]. \tag{1.1}$$

The local random field ξ_n is governed by the discrete stochastic mapping

$$\xi_n = h_n + A(\xi_{n-1}) = f(h_n, \xi_{n-1}) \qquad \xi_0 = 0;\ n = 1, \ldots, N \tag{1.2}$$

where

$$A(x) = (2\beta)^{-1} \ln[\cosh \beta(x+J)/\cosh \beta(x-J)] \tag{1.3}$$

$$B(x) = (2\beta)^{-1} \ln[4 \cosh \beta(x+J) \cosh \beta(x-J)]. \tag{1.4}$$

If the external field h_n is a first-order Markov chain the auxiliary field ξ_n is a second-order Markov chain. The joint probability density $p_n(x, \eta)$ for (ξ_h, h_n) is governed by the Chapman-Kolmogorov equation [3, 4]

$$p_n(x, \eta) = \int d\eta' \int dx'\, T(\eta|\eta') p_{n-1}(x', \eta') \delta(x - f(\eta, x')) \tag{1.5}$$

where $T(\eta|\eta')$ is the transition probability for the external field.

The fixed point of (1.5) gives the invariant measure of the local random field $p^*(x) = \int d\eta\, p^*(x, \eta)$ which can be used to calculate physical quantities like the free energy, the magnetisation, or the Edwards-Anderson parameter [2].

Obviously, the properties of the stochastic mapping depend on the nature of the driving process h_n and on the shape of the function A.

For non-zero temperatures $A(x)$ is infinitely many times differentiable. As a consequence (1.2) generates for a discrete driving process an uncountable number of states. The support of the corresponding invariant measure constitutes for small exchange J a fractal whereas for large J it is continuous [2-7]. Within the fractal range of this support a *physical* quantity, the local magnetisation, exhibits another transition from fractal to continuous behaviour. The corresponding transition line was interpreted to indicate the onset of frustration [5].

For a continuous driving process (without gaps) the support is always the continuum [2, 7, 8].

For zero temperature $A(x)$ is piecewise linear with parts where $\partial_x A(x) = 0$. As a consequence (1.2) generates for a given J only a finite number of possible states so that the theory of finite Markov chains [9] can be applied to determine the invariant measure [3, 4]. The drastic changes in the quality of the support are naturally reflected by the behaviour of its fractal dimension d_f which undergoes, as a function of the physical parameters, continuous as well as discontinuous transitions from one to zero [3, 4, 10] so that d_f behaves similar to order parameters in phase transitions [3, 4, 11]. Due to the non-linearity of A the support is a multifractal which is *topologically* equivalent to the Cantor set but is not in a simple way self-similar. Its fractal dimension can be calculated numerically [10] exploiting methods proposed in [12]. For high temperatures, however, the support can be well approximated by a strictly self-similar Cantor set [3, 4].

Very recently the full scaling properties of the measure have been investigated [13] evaluating a generalised fractal dimension and the spectrum of singularities [14].

In this paper we consider a two-valued first-order Markov chain taking the values $h_\sigma = h_0 + \sigma h$, $\sigma = \pm$, characterised by the probability α that σ changes from lattice site to lattice site,

$$T(\eta|\eta') = \alpha\delta(\eta + \eta' - 2h_0) + (1-\alpha)\delta(\eta - \eta'). \tag{1.6}$$

This choice describes for $\alpha = 0$ a constant external field, for $\alpha = 1$ an alternating field with period one, and for $\alpha = \frac{1}{2}$ the case of uncorrelated (independent identically distributed) variables. For $0 < \alpha < 1$ there exist physical properties which are insensitive to the special value of α whereas others depend on it.

The paper is organised as follows. In § 2 the physical properties at zero temperature are investigated. We determine the possible states of the finite Markov chain and the invariant measure (§ 2.1) which is used to evaluate the magnetisation $\langle m \rangle$ and the residual entropy s_{res} (§ 2.2). We obtain a discontinuous behaviour of these quantities (cf also [15]) dependent on both external field and exchange. For $0 < \alpha < 1$ the location of the discontinuities is independent of α whereas the values of $\langle m \rangle$ and s_{res} depend on α between the discontinuities. This observation can be explained alternatively by simple energy-balance arguments which relate the discontinuities to flips of microscopic spin clusters (§ 2.3).

Section 3 deals with non-zero temperature characteristics of the stochastic mapping. We obtain analytically that the gap which generates the fractal structure of the support vanishes in a linear way if the exchange reaches a critical value in contrast to a recently

proposed $\frac{5}{2}$-power law [16] (§ 3.1). The (always negative) Lyapunov exponent is shown to diverge in the zero-temperature limit. For non-zero temperature we compare results obtained in the Cantor approximation with those of a numerical simulation (§ 3.2). Furthermore, we give a closed analytic expression for the fractal measure in the nth step of the iteration procedure (§ 3.3). In § 4 the application to related models is shortly discussed.

2. Zero-temperature properties

2.1. Support and invariant measure

For zero temperature $A(x)$ is piecewise linear

$$A(x) = \begin{cases} \pm J & \text{for } x \gtrless \pm J \\ x & \text{for } |x| < J. \end{cases} \tag{2.1}$$

As a consequence, for a driving process h_n taking only the values h_σ the mapping (1.2) may generate for the driven process ξ_n only the following states:

$$x(n_+, n_-, 0) = n_+ h_+ + n_- h_- \tag{2.2}$$

$$x(n_+, n_-, \pm J) = n_+ h_+ + n_- h_- \pm J \tag{2.3}$$

where $n_\sigma = 0, 1, \ldots$. All states with $x > J$ and $x < -J$ map after the next iteration into $x = h_\sigma + J$ and $x = h_\sigma - J$, respectively, so that for given physical parameters (h_0, h, J) only a finite number of states (2.2) and (2.3) are generated with n_σ chosen such that

$$x \in [h_+ - J, h_+ + J] \cup [h_- - J, h_- + J]. \tag{2.4}$$

Thus, if the magnetic field takes the value h_i, one of these states, x_i, is generated. Those pairs form the states $z_i = (x_i, h_i)$ of a finite Markov chain. According to the usual classification [9] the states (2.2) are inessential for $0 < \alpha < 1$ because there is a net outflow into the set of essential states (2.3). Thus, for $n \to \infty$ the probability density of the inessential states tends to zero and they should not be taken into account to calculate the invariant measure.

For fixed h the essential states (2.3) (which are independent of the special value of α) build in the (x, h_0, J) space a complicated structure which may be visualised as similar to a honeycomb. In figures 3(a) and 4(a) two cross sections in this space are shown for J = constant and h_0 = constant, respectively. Increasing the variable parameters h_0 and J, the number of states changes in a discontinuous way at some critical values of these parameters which leads to a discontinuous behaviour of physical quantities.

The probability density is the sum of weighted δ functions located at the points $\{x_i, h_i\}$ which constitute the space of states

$$p_n(x, h) = \sum_i w_i^{(n)} \delta(x - x_i) \delta(h - h_i). \tag{2.5}$$

Introducing the vector of weights $\boldsymbol{w}^{(n)} = \{w_i^{(n)}\}$ the Chapman-Kolmogorov equation (1.5) converts, by inserting (2.5), into the matrix equation [3, 4]

$$\boldsymbol{w}^{(n)} = \mathbf{D} \boldsymbol{w}^{(n-1)} \tag{2.6}$$

where the matrix elements of **D** are α if $x_i = f(h_\sigma, x_j = f(h_{-\sigma}, \cdot))$, and are $\gamma = 1 - \alpha$ if $x_i = f(h_\sigma, x_j = f(h_\sigma, \cdot))$, and zero otherwise.

The invariant measure corresponds to the fixed points of (2.6) given by

$$(\mathbf{1} - \mathbf{D})w^* = 0. \tag{2.7}$$

The number of fixed-point solutions is equal to the number of disconnected sets of essential states. For $0 < \alpha < 1$ all essential states are connected and (2.7) has only one fixed point, i.e. the system is ergodic.

To calculate the invariant measure is an exercise in linear algebra. For example, in the range $-h_-/2 < J < h_+/2$ we have for $0 < \alpha < 1$ six essential states $z_i = (x_i, h_i)$ which map applying (1.2) into themselves as shown in the flow diagram in figure 1. $z = \{z_i\}$ and the transition matrix **D** are

$$z = \begin{pmatrix} h_+ + J, h_+ \\ 2h_0 + J, h_+ \\ h_+ - J, h_+ \\ h_- + J, h_- \\ 2h_- + J, h_- \\ h_- - J, h_- \end{pmatrix} \qquad \mathbf{D} = \begin{pmatrix} \gamma & \gamma & \gamma & 0 & 0 & 0 \\ 0 & 0 & 0 & \alpha & 0 & 0 \\ 0 & 0 & 0 & 0 & \alpha & \alpha \\ \alpha & \alpha & \alpha & 0 & 0 & 0 \\ 0 & 0 & 0 & \gamma & 0 & 0 \\ 0 & 0 & 0 & 0 & \gamma & \gamma \end{pmatrix}. \tag{2.8}$$

Obviously, the fixed point of (2.6) depends on α, $w^* = \frac{1}{2}(\gamma, \alpha^2, \gamma\alpha, \alpha, \gamma\alpha, \gamma^2)^T$.

With invariant measures of this type (figure 2) physical quantities are easily calculated.

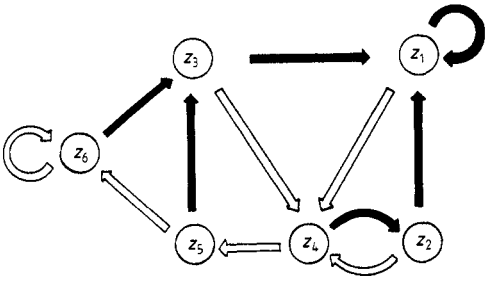

Figure 1. Flow diagram for the six essential states in the region $-h_-/2 < J < h_+/2$. Full and open arrows denote the action of the mapping (1.2) with $h_n = h_+$ and $h_n = h_-$, respectively.

2.2. Residual entropy and magnetisation

The invariant measure allows us to calculate physical quantities such as free energy and magnetisation [2]. For zero temperature the corresponding expressions simplify to

$$f = -\int \mathrm{d}x\, p^*(x) B(x) = -\sum_i w_i^* B(x_i) \tag{2.9}$$

$$\langle m \rangle = \int \mathrm{d}x \int \mathrm{d}y\, p^*(x) p^*(y) \tanh \beta(x + A(y))$$
$$= \sum_{i,j} w_i^* w_j^* \operatorname{sgn}(x_i + A(x_j)). \tag{2.10}$$

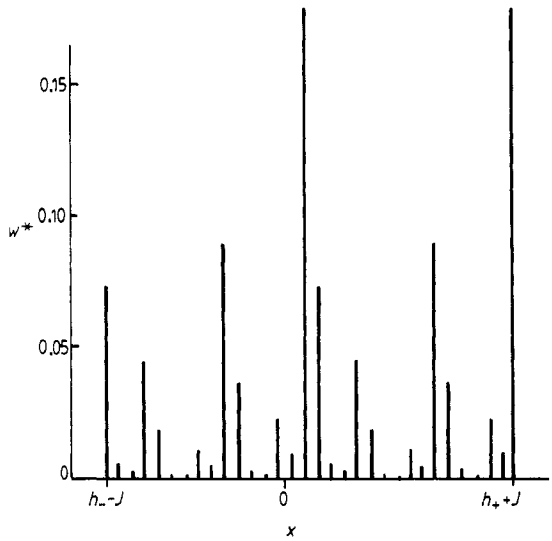

Figure 2. Invariant measure for the 32 essential states for $J = 3h_+/4$, $h_0 = h/4$ (uncorrelated case). In the whole interval $(2h_+ + h_-)/2 < J < h$ the weights remain the same, only the location of the states shifts.

The latter formula is restricted to the uncorrelated case. For zero temperature the function B becomes piecewise linear

$$B(x) = \begin{cases} \pm x & \text{for } x \gtrless \pm J \\ J & \text{for } |x| < J. \end{cases} \tag{2.11}$$

A further quantity of interest, the residual entropy s_{res}, can be directly related to the invariant measure. We start with

$$Z^N = \exp\left(\beta \sum_{n=1}^{N} B(\xi_n)\right) = \prod_{\substack{n=1 \\ \sigma=\pm}}^{N} [2\cosh\beta(\xi_n + \sigma J)]^{1/2} \tag{2.12}$$

which results from (1.1) summing up over the degrees of freedom of the Nth spin. To obtain s_{res} we have to look for terms which give rise to a linear temperature dependence of $f^N = -(\beta N)^{-1} \ln Z^N$. Obviously, the only states which produce this behaviour are $x_i = \pm J$ so that

$$f^N = -(2\beta N)^{-1} \sum_{\substack{n=1 \\ \sigma=\pm}}^{N} \delta_{\xi_n, \sigma J} \ln 2 + o(1/\beta). \tag{2.13}$$

With $s^N = -\partial f^N / \partial T$ we obtain in the thermodynamic limit at zero temperature

$$s_{\text{res}} = \lim_{\beta, N \to \infty} s^N = 2^{-1} k_B (w^*_{x_i = J} + w^*_{x_i = -J}) \ln 2 \tag{2.14}$$

where

$$w^*_{x_i = \sigma J} = \lim_{N \to \infty} N^{-1} \sum_{n=1}^{N} \delta_{\xi_n, \sigma J}.$$

In the following we present explicit results for magnetisation and residual entropy for two cross sections of the above-mentioned honeycomb-like structure in the (x, h_0, J)

space; namely for fixed exchange, $J = h/4$, and for fixed expectation value of the magnetic field, $h_0 = h/4$, respectively (figures 3 and 4). Increasing the variable parameters h_0 and J respectively, the number of states changes in a discontinuous way at some critical values $h_c^{(k)}$ and $J_c^{(k)}$, which leads to a discontinuous behaviour of physical quantities.

For different values of J/h or h_0/h we would obtain different cross sections where, for example, these critical values are shifted. The qualitative picture, however, will not be changed even if we take irrational values.

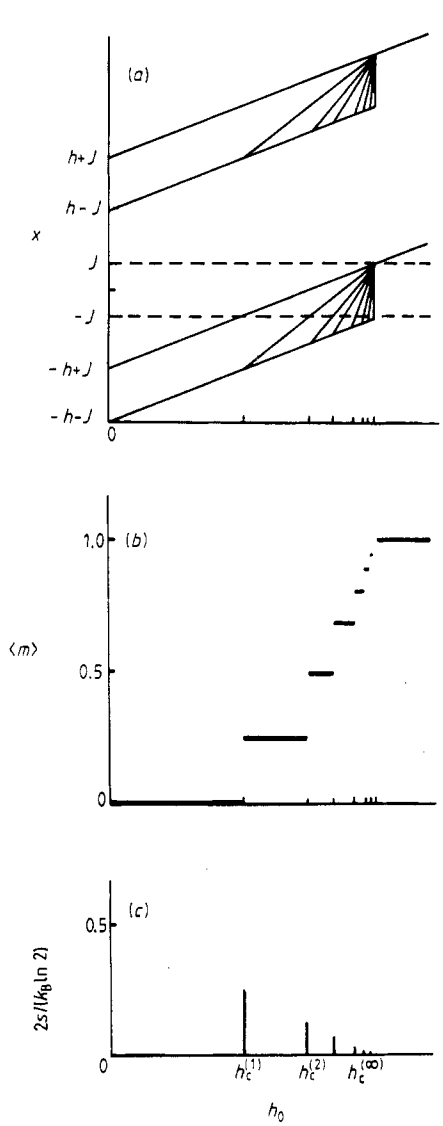

Figure 3. Space of states (a), magnetisation (b), and residual entropy (c) as a function of h_0 for fixed h and $J = h/4$ (uncorrelated case). Only the first six steps and the last one are shown.

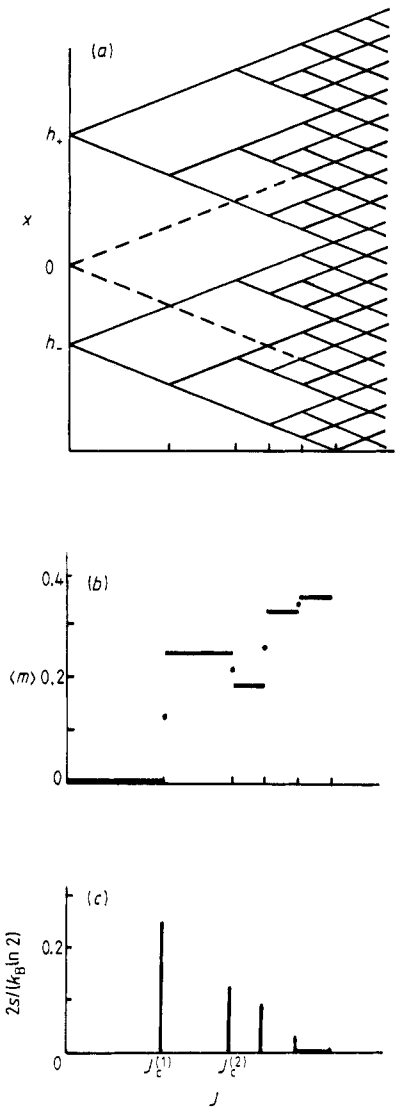

Figure 4. Space of states (a), magnetisation (b) and residual entropy (c) as function of J for fixed h and $h_0 = h/4$ (uncorrelated case). Only the first four steps are shown.

As mentioned above, the essential states are independent of the special value of α in the range $0<\alpha<1$, whereas the invariant measure living on these states depends on it (cf (2.8)). Therefore, the location of the discontinuities does not depend on α but, for example, the altitudes of the steps of $\langle m\rangle$ would depend on α. For simplicity we restrict ourselves, however, to the uncorrelated case.

We first discuss the case of fixed exchange, $J=h/4$ (cf figure 3). Increasing h_0 we find crossing

$$h_c^{(k)}=h-2J/k \qquad k=1,2,\ldots \tag{2.15}$$

that the number of states increases by two and the magnetisation jumps by

$$\Delta m^{(k)}=k(1/2)^{k+1} \qquad \text{with} \qquad \sum_{k=1}^{\infty}\Delta m^{(k)}=1. \tag{2.16}$$

At $h_0=h_c^{(k)}$ the magnetisation is just in the middle between the steps (not shown in figure 3(b)). Furthermore, one of the states crosses the broken lines $x=\pm J$ (cf figure 3(a)) and accordingly the residual entropy has a non-zero value

$$s_{\mathrm{res}}=(1/2)^{k+2}k_{\mathrm{B}}\ln 2. \tag{2.17}$$

The saturation value $\langle m\rangle=1$ is reached for $h_0\geqslant h$ in a monotonous way after an infinite but countable number of jumps. A qualitative behaviour of this kind was already predicted in [15].

Next we discuss the case of a fixed expectation value, $h_0=h/4$ (figure 4). Increasing J the magnetisation jumps at $J_c^{(k)}$ but is *not* monotonically increasing in contrast to the previous case. The values of $J_c^{(k)}$, $\langle m\rangle$, and the residual entropy are given in table 1. We have now a non-zero s_{res} not only at the critical values $J_c^{(k)}$ but also for all $J\geqslant J_c^{(4)}$ since in this range we always have states $x=\pm J$. Accordingly, the magnetisation at $J=J_c^{(k)}$ is for $k>4$, not in the middle between the steps.

The discontinuous behaviour of $\langle m\rangle$ and s_{res} shows that for $T\to 0$ a perturbation theory should fail.

To obtain results for different cross sections requires again the construction of the support and the calculation of the invariant measure along the lines given in § 2.1. Obviously, this could be done on a computer with the help of formula manipulation procedures.

Table 1. Magnetisation and residual entropy as a function of J for $h_0=h/4$. The critical values $J_c^{(k)}$ are defined in the first row.

Range of J	$\langle m\rangle$	$2s_{\mathrm{res}}/(k_{\mathrm{B}}\ln 2)$
$0<J<J_c^{(1)}$	0	0
$J_c^{(1)}=-h_-/2$	2^{-3}	2^{-2}
$J_c^{(1)}<J<J_c^{(2)}$	2^{-2}	0
$J_c^{(2)}=h_+/2$	$7/2^5$	2^{-3}
$J_c^{(2)}<J<J_c^{(3)}$	$3/2^4$	0
$J_c^{(3)}=-h_-$	$33/2^7$	$3/2^5$
$J_c^{(3)}<J<J_c^{(4)}$	$21/2^6$	0
$J_c^{(4)}=(2h_++h_-)/2$	$2793/2^{13}$	2^{-5}
$J_c^{(4)}<J<J_c^{(5)}=h$	$6/17$	$1/510$

2.3. Energy-balance arguments

We demonstrate now how a part of the above results can be alternatively obtained with simple energy-balance arguments and that the discontinuities can be related to flips of microscopic spin clusters. We consider a given realisation of the random magnetic field $\{h_n\}$ and restrict ourselves for simplicity to the uncorrelated case.

2.3.1. Magnetisation against h_0. We suppose that the exchange J is weak enough that for $h_0 = 0$ a given spin s_n will follow the random external field $h_n = \pm h$ even if its two neighbours have the opposite direction. Comparing the energies of the two configurations in figure 5(a) we find the condition $E_1(h_0 = 0) < E_1'(h_0 = 0)$, i.e. $J < h/2$. Since with the same probability $h_n = \pm h$ we have $\langle m \rangle = \lim_{N\to\infty}(1/N)\sum_{n=1}^{N} s_n = 0$.

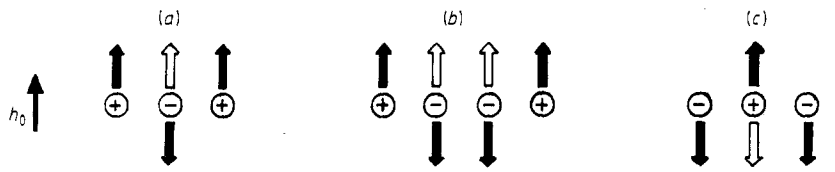

Figure 5. Spin configurations which are responsible for the first few jumps in magnetisation. The spins are subject to the field $h_n = h_\sigma$. The signs denote the value of $\sigma = \pm$ at the corresponding lattice sites. We compare the energies E of the initial configurations (full arrows) with the energies E' of configurations obtained by flipping the inner spins (open arrows).

Switching on a homogeneous external field $h_0 > 0$ changes this situation because up spins are now favoured. The most sensitive configuration is shown in figure 5(a). The down spin flips up if $E_1' < E_1$, i.e. for $h_0 > h_c^{(1)} = h - 2J$. The next threshold $h_c^{(2)} = h - J$ results from clusters of the type shown in figure 5(b). More generally, clusters of k down spins bounded by up spins become unstable at the thresholds $h_c^{(k)}$ given by (2.15). The flips of all down-spin clusters of a given length k at the thresholds $h_c^{(k)}$ lead to a jump of the magnetisation $\Delta m^{(k)}$ given by (2.16) which is equal to $(s_\uparrow - s_\downarrow) \times$ length of the cluster $\times$ probability of the cluster $= 2k(1/2)^{k+2}$. The flipping of shorter down-spin clusters does not influence larger down-spin clusters so that the probabilities can be directly taken from $\{h_n\}$.

At the thresholds the energies of the competing subconfigurations are equal, i.e. the ground state is macroscopically degenerated which is reflected by the non-zero residual entropy (2.17).

2.3.2. Magnetisation against J. Now we would like to apply this line of reasoning to calculate the magnetisation as a function of J for a given value of $h_0 < h$.

We start with $J = 0$ so that each spin s_n will follow the direction of the random external field $h_n = h_\sigma$, and $\langle m \rangle = 0$.

Increasing J favours *parallel* neighboured spins in competition with the random field. The most sensitive subconfiguration is again the single down-spin cluster (figure 5(a)) which becomes unstable for $J > J_c^{(1)} = -h_-/2$. As in the previous case the first jump of magnetisation is $\frac{1}{4}$.

Increasing J further gives, however, a surprise. Now the most sensitive subconfiguration is the single up-spin cluster shown in figure 5(c) which becomes unstable for $J > J_c^{(2)} = h_+/2$. At this threshold the magnetisation decreases. However, the probability of this cluster cannot be simply taken from the initial configuration, since flipping up single down spins *decreases* the number of single up spins (figure 6(a)). From the initial ground state only clusters of five spins shown in figure 6(b) survive, the probability of which is $(1/2)^5$. Thus the jump of the magnetisation at $J_c^{(2)}$ is $-2(1/2)^5 = -1/16$ in accordance with table 1.

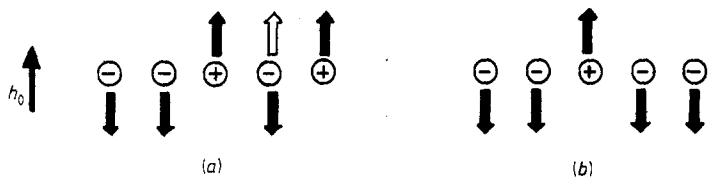

Figure 6. The number of single up-spin clusters (figure 5(c)) is reduced flipping up single down-spin clusters (a). Only subconfigurations (b) survive the reconstruction of the ground state in the region $J_c^{(1)} < J < J_c^{(2)}$.

The third threshold $J_c^{(3)} = -h_-$ originates from the energy-balance condition for two down-spin clusters (figure 5(b)). To calculate the altitude of the third jump as well as the following thresholds and jumps would, however, need an increasing effort at least comparable with our more systematic finite Markov chain analysis.

It is clear that also in the general case the discontinuities of magnetisation are due to flips of microscopic spin clusters. The explanation of the continuous degeneracy of the ground state in this language deserves further investigation.

3. Non-zero temperature properties

3.1. The fractal support

It was previously shown [2-7] that for non-zero temperature the mapping (1.2) generates an uncountable number of essential states. The corresponding invariant measure may have a fractal structure.

These states can be labelled in a kind of symbolic dynamics [17] by sequences of signs which characterise its history [3, 4]. The result of the nth iteration of (1.2) starting from the initial value $\xi_0 = y$ is denoted by

$$x_{\boldsymbol{\sigma}_n;y} = f(h_n, f(h_{n-1}, \ldots, f(h_1, y) \ldots)) \tag{3.1}$$

where $\boldsymbol{\sigma}_n = \{\sigma_n, \ldots, \sigma_1\}$ denotes the sequence of signs corresponding to a given realisation of the driving process $\boldsymbol{h}_n = \{h_{\sigma_n}, \ldots, h_{\sigma_1}\}$. The result of infinitely many iterations (not depending on the initial value since $\partial_x f(h, x) \equiv f' < 1$) is denoted by $x_{\boldsymbol{\sigma}}$ where $\boldsymbol{\sigma}$ symbolises an infinite sequence of signs. The attractor of (1.2), i.e. the support of the invariant measure, is bounded by the fixed points of (1.2) $x_{\boldsymbol{\sigma}}$, $\boldsymbol{\sigma} = \pm$, for constant fields $h_n = h_\sigma = \text{constant}$, $\sigma = \pm$, respectively. These fixed points are

$$x_{\boldsymbol{\sigma}} = h_\sigma/2 + (2\beta)^{-1} \sinh^{-1}[e^{2\beta J} \sinh(\beta h_\sigma)]. \tag{3.2}$$

The hierarchy of gaps can be obtained as mappings of these fixed points [3, 4]. The first gap is $\Delta = x_{+,-} - x_{-,+} = 4h + x_- - x_+$. For $h_0 = 0$ we have $x_+ = -x_- = x^*$, and $\Delta = 2(2h - x^*) = 0$ defines the physical parameters for which the gap disappears. The result for the exchange is well known [2, 5]:

$$J_c = (2\beta)^{-1} \ln[\sinh(3\beta h)/\sinh(\beta h)]. \tag{3.3}$$

For a given J the $(1/\beta, h)$ plane (figure 7) is separated into regions with different signs of the gap by

$$h_c = (2\beta)^{-1} \cosh^{-1}[(e^{2\beta J} - 1)/2]. \tag{3.4}$$

For β_c we do not find an explicit expression, only $\beta_c(h_c = 0) = (2J)^{-1} \ln 3$ results from (3.4).

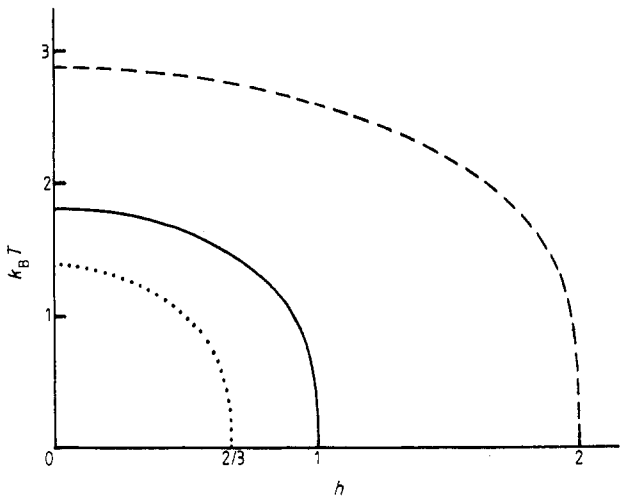

Figure 7. For fixed $J = 1$ the $(1/\beta, h)$ plane is separated into regions with fractal ($\Delta > 0$) and continuous ($\Delta \leqslant 0$) support by (3.4) (full curve). The broken curve corresponds to the onset of frustration. The dotted curve indicates the overlap of bands of the second and third generation.

Since we have the explicit expressions (3.2) and (3.3) we are able to analyse exactly how the gap closes. Expanding x^* near J_c yields

$$x^*(J \to J_c) = 2h + c(J - J_c) \qquad c = \tanh(3\beta h) \tag{3.5}$$

$$\Delta(J \to J_c) = -2c(J - J_c) \tag{3.6}$$

in contrast to the $\frac{5}{2}$-power law which has been claimed to be observed numerically [16] (obviously this is not changed if we multiply (1.2) with β to obtain the mapping considered in [16]).

In [16] it was further claimed that the support is a self-similar Cantor set. The support is, however, a multifractal which is only topologically equivalent to the Cantor set. It can be easily shown that it is not self-similar due to the non-linearity of the mapping. Although the four bands in the second generation have the same width (this is due to the symmetry of the mapping $f(h, -x) = -f(-h, x)$) the eight bands in the third generation have a different width. More precisely, there are two groups of four bands with the same width (figure 8). Only if $A(x) \sim x$, i.e. for a linear mapping do we find a self-similarity on any length scale as it is typical for the Cantor set.

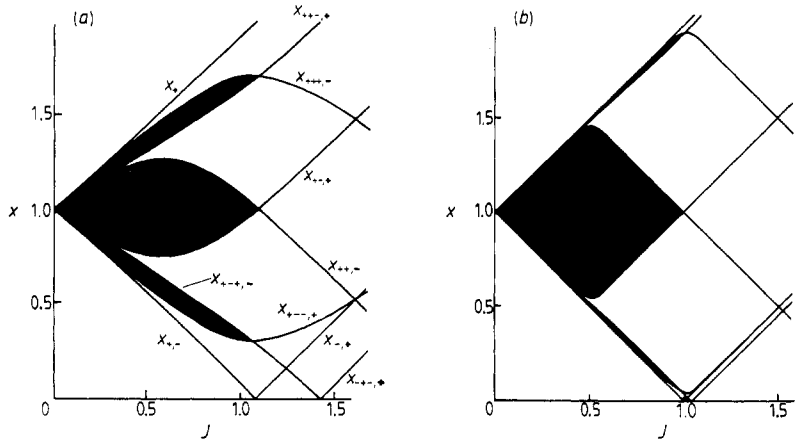

Figure 8. Boundaries of the support and gaps of the second and third generation (black regions) for $x>0$ as function of J for (a) $\beta=1$ and (b) $\beta=10$, for $h_0=0$, $h=1$. For low temperatures the essential states of the zero-temperature case are approached.

In [3, 4] the Cantor approximation was introduced replacing $A(x)$ by $x(x^*-h)/x^*$, i.e. the support was approximated by a strictly self-similar Cantor set, the first gap of which has the exact value. The fractal dimension is

$$d_f^{\text{Cantor}}=\begin{cases}1 & \text{if } \Delta\leqslant 0\\ \ln 2/\ln[x^*/(x^*-h)] & \text{if } \Delta>0.\end{cases} \tag{3.7}$$

Near the critical exchange we find with (3.5) that

$$d_f^{\text{Cantor}}(J\to J_c)=1-(c/2h\ln 2)(J_c-J). \tag{3.8}$$

The Cantor approximation works well for high temperatures and is an analytic approximation which ensures the correct behaviour of the first gap.

If $d_f=1$ the support is continuous but the measure constitutes a fat fractal which may be characterised by different characteristic quantities [18].

A physical quantity, the local magnetisation, given by $m=\langle s_i\rangle=\tanh\beta(x+A(x'))$ where both x and x' are governed by the invariant measure p^* [2], also exhibits a transition from fractal to continuous behaviour [5]. Continuous values become possible if $m=0$ is not excluded, i.e. for $x_{-,+}+A(x_+)\geqslant 0$ which yields $e^{2\beta J}\geqslant 2\cosh(\beta h)$. This transition line (figure 7) was interpreted to indicate the onset of frustration [5] since for $m=\langle s_i\rangle=0$ no direction of s_i is preferred which means a 'remis' in the competition between exchange and local random field. It terminates for $T=0$ at $h/J=2$ where the residual entropy first becomes non-zero.

The overlap of bands of different generations defines further lines in the $(1/\beta, h)$ plane which terminate for *zero temperature* at $h=2J/k$, $k=3,4,\ldots$. These are just the values for which the number of essential states jumps by two and the residual entropy exhibits spikes. For instance, bands of second and third generation overlap if $x_{++,-}=x_{-,+}$ which gives the zero temperature $h=2J/3$ (figure 7).

3.2. The Lyapunov exponent

For non-zero temperature we have $f'<1$ so that it is clear from the very beginning

that the mapping is non-chaotic and that the Lyapunov exponent is negative,

$$\lambda = \int \mathrm{d}x\, p^*(x) \ln f'(x) < 0. \tag{3.9}$$

For zero temperature we have $f' = 1$ for $|x| < J$ and zero otherwise. The support, however, is the interval $[-h-J, h+J]$ so that the integration yields

$$\lambda(\beta \to \infty) = -\infty. \tag{3.10}$$

The Lyapunov exponent is a measure of the convergence of two trajectories corresponding to the same realisation of the driving process starting with different initial values y and y'. $\lambda < 0$ corresponds to

$$\lim_{n\to\infty} |x_{\sigma_n,\ldots y} - x_{\sigma_n,\ldots y'}| = 0. \tag{3.11}$$

Roughly speaking, the convergence is faster the 'fewer' states are at our disposal. For $\beta \to \infty$ the space of states collapses to a finite number of states and $\lambda = -\infty$.

In the Cantor approximation we have $f' = (x^* - h)/x^* = \text{constant}$, and with $\int \mathrm{d}x\, p^*(x) = 1$ we find the Lyapunov exponent

$$\lambda^{\text{Cantor}} = \ln[(x^* - h)/x^*]. \tag{3.12}$$

For $d_f \leqslant 1$ we can write $\lambda^{\text{Cantor}} = -\ln 2/d_f^{\text{Cantor}}$ which makes it clear that the convergence is faster the sparser is the support. If the first gap closes $d_f \to 1$. Inserting (3.8) we find

$$\lambda^{\text{Cantor}}(J \to J_c) = -\ln 2 + (c/2h)(J - J_c). \tag{3.13}$$

In figure 9 results of a numerical simulation are compared with those of the Cantor approximation.

3.3. The measure

In [2] the shape of the measure was illustrated by a numerical iteration of the Chapman-Kolmogorov equation. Similar pictures are generated by Monte Carlo

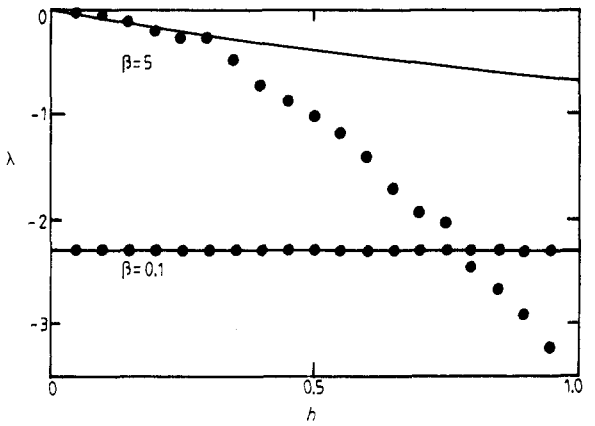

Figure 9. Lyapunov exponent ($h_0 = 0$, $J = 1$) as a function of h for different temperatures obtained by numerical simulation (full circles) and in the Cantor approximation (full lines). For high temperatures the results practically coincide.

simulations [7]. In [4] it was shown that starting from a non-trivial initial measure the iteration of (1.5) converges to a unique fixed point p^*. Here we give a systematic prescription of how to obtain an analytic expression in the nth step of the iteration procedure. For simplicity we restrict ourselves to the uncorrelated case, the generalisation to $\alpha \neq \frac{1}{2}$ is straightforward.

We start with a normalised initial measure $p_0(x)$ which is non-zero only in the interval $I=[x_-, x_+]$ which contains the support. To evaluate the first iteration of (1.5) with $T(\eta|\eta')$ given by (1.6)

$$p_1(x)=\int \mathrm{d}x'\, p_0(x') \sum_{\sigma=\pm} \delta(x-f(h_\sigma, x'))/2 \tag{3.14}$$

we exploit that $x_{\sigma;y}=f(h_\sigma, y)$ has the monotonic inversion

$$y_{\sigma;x}=f^{-1}(h_\sigma, x)=-(2\beta)^{-1}\ln[\sinh\beta(J-x+h_\sigma)/\sinh\beta(J+x-h_\sigma)] \tag{3.15}$$

so that $\delta(x-f(h,x'))=|\partial_{x'}f(h,x')|^{-1}\delta(x'-f^{-1}(h,x))$. The prefactor of the δ function is

$$W(x')=|2\cosh\beta(x'+J)\cosh\beta(x'-J)/\sinh(2\beta J)|. \tag{3.16}$$

Thus we obtain from (3.14) that

$$p_1(x)=\begin{cases} p_\sigma(x)=p_0(y_{\sigma;x})\,W(y_{\sigma;x})/2 & \text{for } x\in x_{\sigma;I} \\ 0 & \text{otherwise} \end{cases} \tag{3.17}$$

where $W(y_{\sigma;x})=|\sinh(2\beta J)/[2\sinh\beta(J-x+h_\sigma)\sinh\beta(J+x-h_\sigma)]|$. In this way $p_0(x)$ generates two bands p_σ living on the mappings of the initial support $x_{\sigma;I}=[x_{\sigma,-}, x_{\sigma,+}]$.

In the nth step we have 2^n bands which can be labelled by the sequence of n signs $\boldsymbol{\sigma}_n$ characterising its history. A band $p_{\boldsymbol{\sigma}_{n-1}}(x)$ living on $x_{\boldsymbol{\sigma}_{n-1};I}$ generates in the next iteration the two bands

$$p_{\boldsymbol{\sigma}_n}(x)=p_{\boldsymbol{\sigma}_{n-1}}(y_{\sigma_n;x})\,W(y_{\sigma_n;x})/2 \qquad x\in x_{\boldsymbol{\sigma}_n;I}. \tag{3.18}$$

Denoting the result of n inversions (cf (3.1)) by

$$y_{\boldsymbol{\sigma}_n;x}=f^{-1}(h_1, f^{-1}(h_2, \ldots, f^{-1}(h_n, x)\ldots)) \tag{3.19}$$

we obtain from (3.17) and (3.18) the closed expression

$$p_{\boldsymbol{\sigma}_n}(x)=p_0(y_{\boldsymbol{\sigma}_n;x})\prod_{\nu=1}^{n}[W(y_{\boldsymbol{\sigma}_\nu;x})/2] \qquad x\in x_{\boldsymbol{\sigma}_n;I}. \tag{3.20}$$

The measure in the nth generation consists of 2^n bands labelled by the 2^n possible sequences of n signs $\pm$. The explicit expression (3.20) may be helpful to characterise the fractal measure calculating generalised scaling exponents [14, 18].

We observed that for $0<J<-h_-/2$ already the second iteration reproduces the zero-temperature limit

$$p(x)=\tfrac{1}{4}[\delta(x-h_++J)+\delta(x-h_-+J)+\delta(x-h_+-J)+\delta(x-h_--J)]$$

which corresponds to the fact that in this range, for $\alpha=\frac{1}{2}$, $\lim_{n\to\infty} D^n=D^2$ (cf (2.6)).

Whereas for zero temperature the number of states jumps, crossing some critical parameters (which causes a discontinuous behaviour of physical quantities), for non-zero temperature we have at a given step of the iteration procedure always the same

number of bands given by the same analytic expression. Therefore we expect that for the latter case the discontinuous behaviour will be smoothed and no phase transition will occur in accordance with the general arguments for 1D systems.

In [16] it was claimed that even if the gap is closed 'quasibands' can be seen, the number of which increases by one at critical values of the exchange. We stress, however, that for a fractal structure statements of this kind make no sense without a reference to a relevant length scale (e.g., in figure 3(a) of [16] one sees four bands or eight bands or even more depending on the reference length).

4. Concluding remarks

It is obvious that related models such as the random-exchange Ising chain ($J_n = \pm J$) can be treated by adapting this formalism. For non-zero temperature the corresponding mapping, $\xi_n = h + A(\xi_{n-1})\ \mathrm{sgn}\ J_n$, generates a fractal structure the gap of which disappears at $x^* = 2h$ as for the random-field Ising chain [2]. For zero temperature this mapping generates again only a finite number of essential states $x(m, \pm J) = mh \pm J$, $m = 0, \pm 1, \pm 2, \ldots$, chosen such that $x \in [h - J, h + J]$. We applied the theory of finite Markov chains to determine the invariant measure and recovered in this way easily the results for magnetisation obtained in [15] with a different method (cf figure 2(b) in [15] for the uncorrelated case).

A further possible application of this formalism would be the Ising chain in a quasiperiodic two-valued magnetic field where for zero temperature a discontinuous behaviour of magnetisation and a non-trivial residual entropy have also been observed [19]. In this case one would have to calculate a deterministic measure corresponding to an infinite sequence of signs (generated from a finite sequence by some recursion relation) which characterises the geometry of the model.

Acknowledgment

The authors would like to thank Slava Priezzhev for valuable discussions.

References

[1] Rujan P 1978 *Physica* **91A** 549
[2] Györgyi G and Rujan P 1984 *J. Phys. C: Solid State Phys.* **17** 4207
[3] Behn U and Zagrebnov V A 1987 *J. Stat. Phys.* **47** 939
[4] Behn U and Zagrebnov V A 1987 *JINR Dubna* E17-87-138
[5] Bruinsma R and Aeppli G 1983 *Phys. Rev. Lett.* **50** 1494
[6] Aeppli G and Bruinsma R 1983 *Phys. Lett.* **97A** 117
[7] Normand J M, Mehta M L and Orland H 1985 *J. Phys. A: Math. Gen.* **18** 621
[8] Andelman D 1986 *Phys. Rev.* B **34** 6214
[9] Kemeny J G and Snell J L 1983 *Finite Markov Chains* (Berlin: Springer)
[10] Szepfalusy P and Behn U 1987 *Z. Phys.* B **65** 337
[11] Badii R and Politi A 1987 *Phys. Scr.* **35** 243
[12] Szepfalusy P and Tel T 1986 *Phys. Rev.* A **34** 2520
[13] Evangelou S N 1987 *J. Phys. C: Solid State Phys.* **20** L511
[14] Halsey T C, Jensen M H, Kadanoff L P, Procaccia I and Shraiman B I 1986 *Phys. Rev.* A **33** 1141

[15] Derrida D, Vannimenus J and Pomeau Y 1978 *J. Phys. C: Solid State Phys.* **11** 4749
[16] Satija I I 1987 *Phys. Rev.* B **35** 6877
[17] Guckenheimer J and Holmes P 1986 *Nonlinear Oscillations, Dynamical Systems and Bifurcations of Vector Fields* (Berlin: Springer)
[18] Eykholt R and Umberger D K 1986 *Phys. Rev. Lett.* **57** 2333
[19] Luck J M 1987 *J. Phys. A: Math. Gen.* **20** 1259